


SHORT COMMUNICATION

Open Access



# The phosphoethanolamine transferase PetL of *Pasteurella multocida* is associated with colistin resistance

Jie Yang<sup>1,2,3</sup>, Lin Lin<sup>1,2,3</sup>, Haixin Bi<sup>1,2,3</sup>, Congcong Shi<sup>1,2,3</sup>, Qingjie Lv<sup>1,2,3</sup>, Lin Hua<sup>1,2,3</sup>, Huanchun Chen<sup>1,2,3</sup>, Bin Wu<sup>1,3\*</sup> and Zhong Peng<sup>1,2,3\*</sup> 

## Abstract

The rapid emergence and spread of colistin-resistant gram-negative bacteria has raised worldwide public health concerns, and phosphoethanolamine (PEtn) transferase modification-mediated colistin resistance has been widely documented in multiple gram-negative bacterial species. However, whether such a mechanism exists in the zoonotic pathogen *Pasteurella multocida* is still unknown. Recently, a novel PEtn transferase, PetL, was identified in *P. multocida*, but whether it is associated with colistin resistance remains to be elucidated. In this study, we found that PetL in *P. multocida* (PetL<sup>PM</sup>) exhibited structural characteristics similar to those of the mobile-colistin-resistant (MCR) protein and the PEtn transferase characterized in *Neisseria meningitidis*. The transformation of *petL*<sup>PM</sup> into *E. coli* or *K. pneumoniae* changed the phenotype of several tested strains from colistin sensitive to colistin resistant. Deletion of this gene decreased the colistin minimum inhibitory concentration (MIC) of *P. multocida* by 64-fold. Our extensive analysis by MALDI-TOF-MS demonstrated that PetL<sup>PM</sup> participated in the modification of bacterial lipopolysaccharide (LPS)-lipid A. Deletion of *petL*<sup>PM</sup> led to an increase in membrane charge but a decrease in cell-surface hydrophobicity and cell permeability in *P. multocida*. The present study is the first to report the presence of PEtn transferase-mediated colistin resistance in the zoonotic pathogen *P. multocida*.

**Keywords** Antimicrobial resistance, Colistin, *Pasteurella multocida*, Phosphoethanolamine transferase, Lipid A modification

## Introduction

The spread of drug-resistant bacteria, including multi-drug-resistant (MDR), extensive drug-resistant (XDR), and pandrug-resistant (PDR) bacteria, poses serious threats to global public health (Walsh et al. 2023). The World Health Organization (WHO) has listed several antimicrobials as critically important agents for human medicine (WHO 2023). Notably, colistin has been recognized as a “last-resort” antibiotic for treating infections associated with MDR gram-negative bacteria (Sharma et al. 2022). As a positively charged polycationic peptide, colistin mainly works by interacting with negatively charged phosphate groups of bacterial lipopolysaccharide (LPS)-lipid A, thereby disrupting bacterial permeability

Handling Editor: Yuan Liu (Associate Editor).

\*Correspondence:

Bin Wu

wub@mail.hzau.edu.cn

Zhong Peng

pengzhong@mail.hzau.edu.cn

<sup>1</sup> National Key Laboratory of Agricultural Microbiology, College of Veterinary Medicine, Huazhong Agricultural University, Wuhan, China

<sup>2</sup> Hubei Hongshan Laboratory, Wuhan, China

<sup>3</sup> Frontiers Science Center for Animal Breeding and Sustainable Production, The Cooperative Innovation Center for Sustainable Pig Production, Wuhan, China



© The Author(s) 2024. **Open Access** This article is licensed under a Creative Commons Attribution 4.0 International License, which permits use, sharing, adaptation, distribution and reproduction in any medium or format, as long as you give appropriate credit to the original author(s) and the source, provide a link to the Creative Commons licence, and indicate if changes were made. The images or other third party material in this article are included in the article's Creative Commons licence, unless indicated otherwise in a credit line to the material. If material is not included in the article's Creative Commons licence and your intended use is not permitted by statutory regulation or exceeds the permitted use, you will need to obtain permission directly from the copyright holder. To view a copy of this licence, visit <http://creativecommons.org/licenses/by/4.0/>. The Creative Commons Public Domain Dedication waiver (<http://creativecommons.org/publicdomain/zero/1.0/>) applies to the data made available in this article, unless otherwise stated in a credit line to the data.

and leading to bacterial lysis (Poirel et al. 2017). In recent years, the worldwide increase in the emergence and dissemination of colistin-resistant bacteria, particularly those harboring the plasmid-borne mobile-colistin-resistant (MCR) gene *mcr* (Liu et al. 2016), has raised a global public health concern (Seethalakshmi et al. 2023). In addition, a chromosome-borne phosphoethanolamine (PEtn) transferase, which plays a role in modifying LPS lipid A by adding PEtn residues, has also been found to be associated with colistin resistance in several bacterial species, including *Neisseria meningitidis*, *Acinetobacter baumannii* and *Vibrio parahaemolyticus* (Huang et al. 2018). The mechanisms associated with colistin resistance in other gram-negative bacteria remain to be explored due to the importance of this agent in combating infections.

The Gram-negative zoonotic pathogen *Pasteurella multocida* is a leading cause of multiple economic-impact diseases in agriculture (Wilkie et al. 2012; Wilson and Ho 2013). Infections from this agent may also lead to pneumonia and other respiratory disorders, bacteremia, meningitis, sepsis, and even peritonitis in humans (Piorunek et al. 2023). In recent years, the morbidity and mortality of human Pasteurellosis have increased worldwide (Wilson and Ho 2013). This is partly due to the rapid increase in populations of companion animals (e.g., dogs and cats) and food-producing animals (e.g., pigs and cattle) worldwide to meet the nutrient and spiritual demands of humans (Peng et al. 2022). Because *P. multocida* commonly exists in the upper respiratory tracts of these animal species, and animal exposure, particularly biting, scratching and even licking companion animals, is the primary reason for humans acquiring pasteurellosis (Wilson and Ho 2013). Although data regarding colistin resistance in *P. multocida* are relatively scarce, several recent studies from other groups have shown that *P. multocida* strains originating from avians and ruminants exhibit high levels (between 60 and 70%) of resistance to colistin (El-Demerdash et al. 2023; Sebbar et al. 2020). However, the related mechanism remains to be elucidated. Recently, a novel PEtn-transferase, PetL, was identified in *P. multocida* (PetL<sup>PM</sup>), and it is likely to play a role in transferring PEtn to LPS-lipid A (Harper et al. 2017). The aim of this study was to investigate whether PetL<sup>PM</sup> is associated with colistin resistance.

## Results

### *P. multocida* PetL is associated with colistin resistance

Considering that there is no breakpoint available for the interpretation of colistin resistance in *P. multocida*, we amplified the full-length of the *petL* gene from *P. multocida* HuN001 (GenBank accession no. CP073238) and cloned this gene (*petL*<sup>PM</sup>) into different plasmids,

followed by transformation of the constructed *petL*<sup>PM</sup>-bearing plasmids into different *Klebsiella pneumoniae* and *Escherichia coli* strains. Measurement of the minimal inhibitory concentration (MIC) of colistin on *E. coli* or *K. pneumoniae* strains containing *petL*<sup>PM</sup>-bearing plasmids or empty plasmids through the broth microdilution method showed that the transformation of *petL*<sup>PM</sup> led to an increase in the colistin MIC (Fig. 1A, B). In *E. coli*, the transformation of *petL*<sup>PM</sup> caused increases of 16- and 64-fold in the colistin MICs, respectively (Fig. 1A). In *K. pneumoniae*, this process induced increases of 4- and 16-fold, respectively (Fig. 1B). The phenotype of several tested strains changed from colistin sensitive to colistin resistant after *petL*<sup>PM</sup> transformation, as interpreted using the Clinical & Laboratory Standards Institute (CLSI) breakpoint for colistin (2 µg/mL). We next knocked out *petL* from HuN001 and measured the MIC of colistin on the *petL*-deletion strain (PM-Δ*petL*), the wild-type strain (PM-WT), and the *petL*-complementary strain (PM-C*petL*). The results demonstrated that the deletion of *petL* led to a 64-fold decrease in the colistin MIC in *P. multocida* (PM-WT vs. PM-Δ*petL*: 2 µg/mL vs. 0.03125 µg/mL; Fig. 1C). Measurement of growth conditions showed that the deletion of *petL* did not affect the growth of *P. multocida* (Fig. 1D). The above findings indicated that *P. multocida* PetL was associated with colistin resistance.

### *P. multocida* PetL participates in the modification of the bacterial LPS lipiddA

To understand the working mechanism of PetL<sup>PM</sup>, we predicted the structure of PetL<sup>PM</sup> and compared it to the structures of MCR-1 (PDB ID code 5GOV) and PetL in *N. meningitidis* (Pet<sup>NM</sup>; PDB ID code 5FGN). The results demonstrated that PetL<sup>PM</sup> was an integral membrane protein with 5 N-terminal transmembrane helices (Fig. 2A). This topological characteristic was similar to that of MCR-2 (Sun et al. 2017). The predicted structure was highly homologous to that of MCR-1 (Fig. 2B) and Pet<sup>NM</sup> (Fig. 2C). These findings suggest that PetL<sup>PM</sup> may work through a similar mechanism to that of MCR. We therefore transformed *petL*<sup>PM</sup> into *E. coli* MG1655 with the help of a *P. multocida*-*E. coli* shuttle vector pPBA1101 and isolated LPS-lipid A from MG1655 harboring *petL*<sup>PM</sup> (MG1655-*petL*<sup>PM</sup>) as well as MG1655 with (MG1655-pPBA) or without (MG1655) the empty vector pPBA1101 for analysis by MALDI-TOF-MS using the same model and analysis methodology for the functional characterization of MCR-2 (Sun et al. 2017). Lipid A modification signaling was detected in MG1655-*petL*<sup>PM</sup> but not in MG1655-pPBA or MG1655 (Fig. 3). We also isolated LPS-lipid A from PM-WT and PM-Δ*petL* for extensive analysis by MALDI-TOF-MS, but this

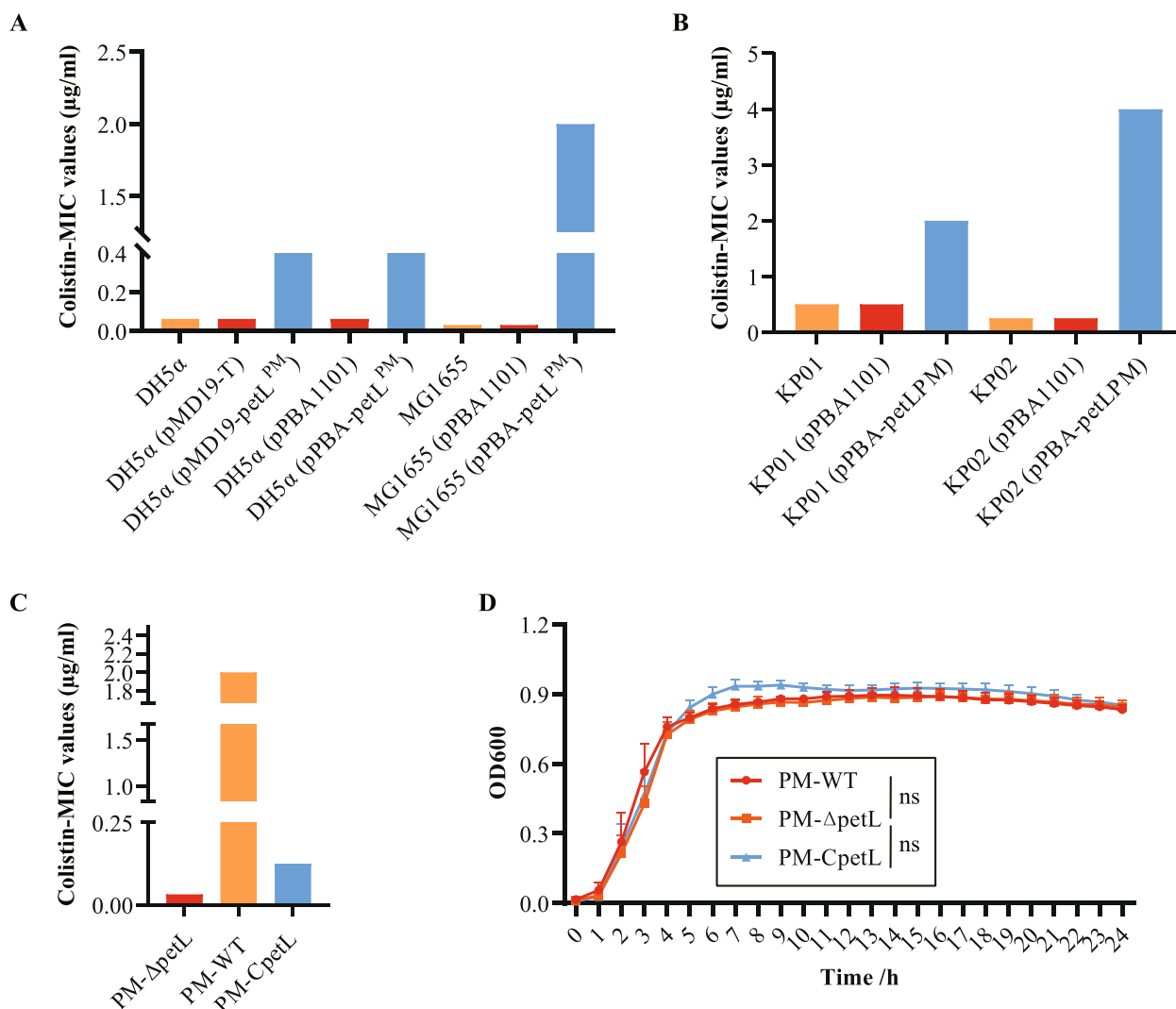


**Fig. 1** Influence of the phosphoethanolamine transferase PetL on the colistin susceptibility of *Pasteurella multocida*. **A** A column chart showing the minimal inhibitory concentration (MIC) values of colistin on different *E. coli* strains containing plasmid-bearing *petL* from *P. multocida* or with or without the corresponding plasmids; **B** A column chart showing the MIC values of colistin on different *Klebsiella pneumoniae* strains containing plasmid-bearing *petL* from *P. multocida* or with or without the corresponding plasmids; **C** A column chart showing the minimal inhibitory concentration (MIC) values of colistin on the *P. multocida* wild type strain (PM-WT), *petL* deletion strain (PM-ΔpetL), and *petL* complementary strain (PM-CpetL); **D** A line chart showing the OD<sub>600</sub> values of the *P. multocida* wild type strain (PM-WT), *petL* deletion strain (PM-ΔpetL), and *petL* complementary strain (PM-CpetL) in TSB media at different time points

approach still did not provide any indicative results from the mass data obtained.

***P. multocida* PetL plays a role in maintaining bacterial membrane charge, cell surface hydrophobicity, and cell permeability**

Considering the important role of the electrostatic interaction between the positively charged colistin and the negatively charged gram-negative bacterial lipid A in the work of colistin (Poirel et al. 2017), we measured the surface negative charge of different *P. multocida* strains

using FITC-labeled poly-L-lysine. More negative surface charges (increased 10.55%) were detected in PM-ΔpetL than in PM-WT (Fig. 4A). In transformed *E. coli* strains with different *petL*<sup>PM</sup>-bearing plasmids, the number of negative surface charges (DH5α (pPBA-1101) decreased by 12.24% compared to that of DH5α (pPBA-petL)), and DH5α (pMD19-T) decreased by 8.76% compared to that of DH5α (pMD19-petL) compared to that of the control strains (Fig. 4B). Measurement of cell-surface hydrophobicity revealed that PM-ΔpetL displayed lower cell-surface hydrophobicity (decreased 19.5%)

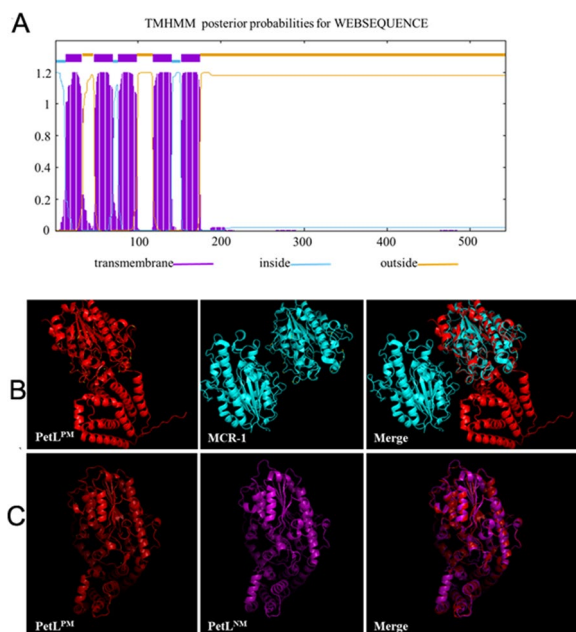


**Fig. 2** Predicted structural characteristics of the phosphoethanolamine transferase PetL in *Pasteurella multocida*. **A** Structural characteristics of PetL in *P. multocida* predicted by the TMHMM server V. 2.0; **B** predicted structure of PetL in *P. multocida* and its comparison with the structure of MCR-1 (ID code 5GOV); **C** predicted structure of PetL in *P. multocida* and its comparison with the structure of PetL characterized in *Neisseria meningitidis* (PetL<sup>NM</sup>; ID code 5FGN)

than PM-WT (Fig. 4C). In addition, PM- $\Delta$ petL exhibited decreased cell permeability (20.71% lower) compared with that of PM-WT (Fig. 4D).

## Discussion

As an important “last-resort” antibiotic, colistin is crucial for combating MDR-gram-negative bacteria, and the emergence of bacterial agents with decreased susceptibility to colistin has raised great public health concerns worldwide (Seethalakshmi et al. 2023). Although methodological difficulties hampering the analysis of susceptibility to colistin have led to relatively scarce data on colistin resistance in *P. multocida* (Kempf et al. 2016), several recent studies have shown that *P. multocida* strains originating from avians and ruminants exhibit high levels (between 60 and 70%) of resistance to colistin (El-Demerdash et al. 2023; Sebbar et al. 2020). These findings suggest that colistin resistance might also be a problematic phenotype in *P. multocida*. We believe that the susceptibility profiles of *P. multocida* to colistin should not be ignored due to the potential public health risks of this bacterial species (Peng et al. 2022). Considering that the treatment of human pasteurellosis mainly relies on the administration of antibiotics (Wilson and Ho 2013) and

the susceptibility of *P. multocida* to many antimicrobial agents is decreasing (Michael 2018), colistin may play a key role in treating human pasteurellosis caused by MDR-*P. multocida* in specific cases, and exploring the mechanisms associated with colistin resistance in this zoonotic bacterial species is therefore of clinical significance.

In this study, we demonstrated that the newly characterized PEtn transferase PetL (Harper et al. 2017) is associated with colistin resistance, and our bioinformatics analysis revealed that PetL<sup>NM</sup> exhibited structural characteristics similar to those of both MCR-1 and PetL<sup>PM</sup>. Notably, the roles of PetL<sup>NM</sup> and MCR-1 in conferring colistin resistance have been fully clarified in *N. meningitidis* and *Enterobacteriaceae*, respectively (Liu et al. 2016; Anandan et al. 2017). Therefore, the working mechanism by which PetL<sup>PM</sup> mediates colistin resistance might also be similar to that of both MCR-1 and PetL<sup>NM</sup>. According to published articles (Sun et al. 2017; Anandan et al. 2017), both MCR proteins and PetL<sup>NM</sup> are indeed PEtn transferases and play roles in modifying lipid A by transferring PEtn from its primary phosphatidylethanolamine, and this role of several MCR proteins, such as MCR-2, has been experimentally demonstrated in the *E. coli* MG1655 model using MALDI-TOF-MS (Sun et al. 2017). Using the same model and analysis methodology, a clear curve reflecting lipid A modification in MG1655 containing *petL*<sup>PM</sup> was observed in this study. However, we did not obtain any indicative results from the mass data generated by MALDI-TOF-MS analysis of LPS-lipid A from PM-WT, PM- $\Delta$ petL or PM-CpetL. This might be because the structure of LPS of *P. multocida* is complex (Harper and Boyce 2017; Harper et al. 2011), and there is still a lack of reference data for the analysis. However, it is noteworthy that a recent study experimentally verified the role of PetL in transferring PEtn to lipid A in *P. multocida* (Harper et al. 2017). It is known that PEtn residues are positively charged; the deletion of PetL reduces the transformation of the positively charged PEtn to bacterial lipid A, and the bacterial surface-negative charge might therefore increase. This could explain why PM- $\Delta$ petL possessed more negative charges than did PM-WT. An increase in the surface negative charge of PM- $\Delta$ petL might be beneficial for the binding of positively charged colistin (Poirel et al. 2017). In addition, PM- $\Delta$ petL exhibited decreased cell permeability compared with that of PM-WT. The above changes may contribute to the decreased bactericidal activity of colistin, possibly explaining why PM- $\Delta$ petL had a lower colistin MIC than PM-WT.

In conclusion, we demonstrated that the newly identified PEtn transferase PetL of *P. multocida* is associated with colistin resistance. The present study is the first to report the presence of PEtn transferase-mediated colistin resistance in the zoonotic pathogen *P. multocida*. Although colistin is currently not frequently used for

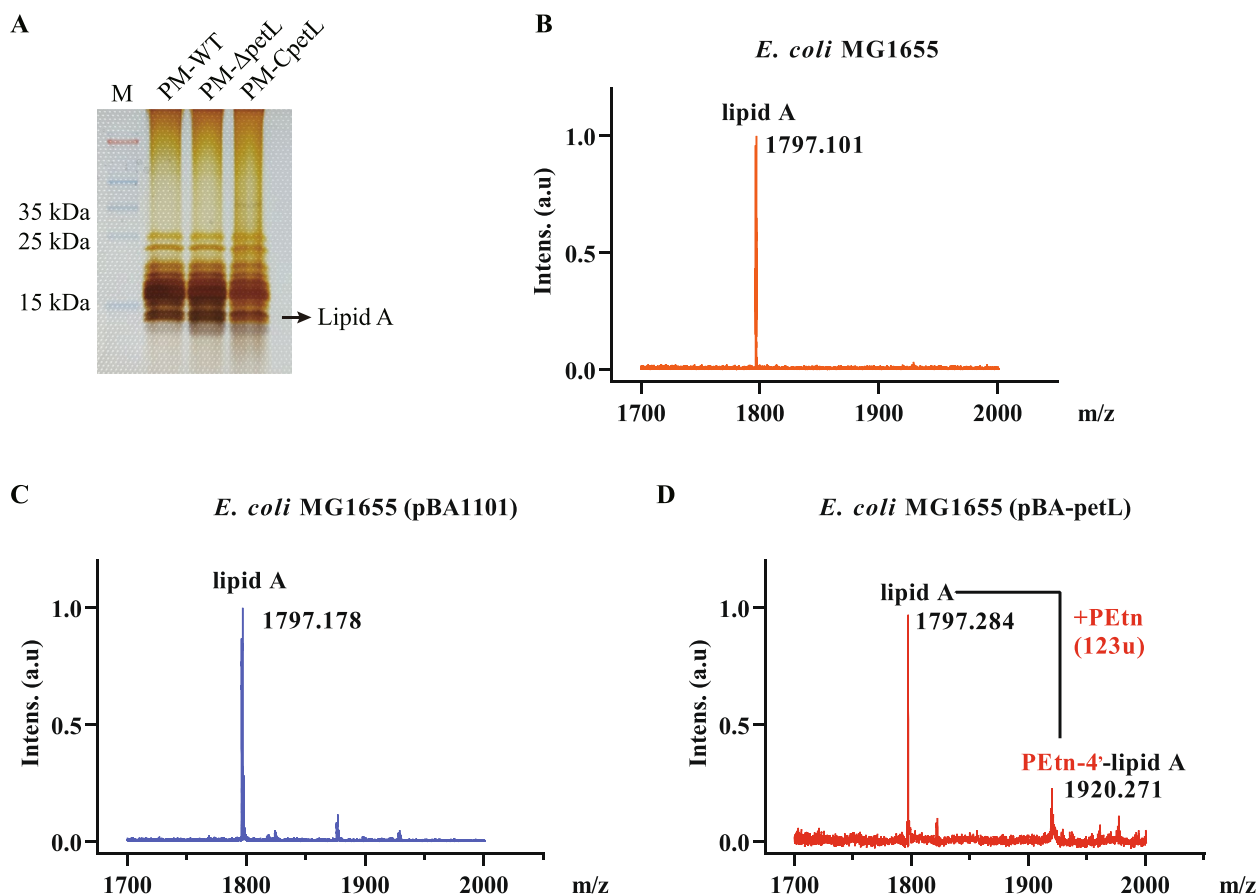


**Fig. 3** Analysis of *Pasteurella multocida* lipopolysaccharide (LPS) and lipid A. **A** Separation of LPS extracted from *P. multocida* strain HuN001 by SDS polyacrylamide gel electrophoresis (SDS-PAGE); **B** Matrix-assisted laser desorption ionization time-of-flight mass spectrometry (MALDI-TOF-MS) analysis of lipid A extracted from *E. coli* MG1655; **C** MALDI-TOF-MS analysis of lipid A extracted from *E. coli* MG1655 containing plasmid pBA1101; **D** MALDI-TOF-MS analysis of lipid A extracted from *E. coli* MG1655 containing *petL* from *P. multocida* HuN001 carried by plasmid pBA1101

the treatment of *P. multocida* infections in clinical practice, our study still provides information on the selection of colistin when necessary. This might also be important due to the zoonosis of this bacterial species, as the rapid increase in the population of pets worldwide may increase the public risk of *P. multocida* in the future.

## Materials and methods

### Bacterial strains, plasmids, and bioinformatics analysis

The bacterial strains and plasmids used in this study are listed in Table 1. Unless otherwise specified, *P. multocida* strains were cultured as described previously (Lv et al. 2023). *K. pneumoniae* and *E. coli* strains were incubated in Luria–Bertani (LB) broth (Sigma–Aldrich, St. Louis, US) or in agar at 37°C. When necessary, kanamycin (100 µg/mL) was given to the medium-cultured bacterial strains containing plasmid pBA1101 (gifted by Prof. John D. Boyce), while ampicillin (100 µg/mL) was used for the culture of bacterial strains containing pMD<sub>19</sub>-T.

The putative structure of PetL<sup>PM</sup> was predicted using the I-TASSER server (<https://seq2fun.dcmdb.med.umich.edu/I-TASSER/>). The crystal structures of MCR-1 (ID code 5GOV) and PetL in *N. meningitidis* (PetL<sup>NM</sup>; ID code 5FGN) were downloaded from the PDB database ([www.pdb.org](http://www.pdb.org)). Protein structures were compared using PyMOL 2.0 (<https://pymol.org/2/>). The characteristics of PetL<sup>PM</sup> were analyzed using the TMHMM server V. 2.0 (<http://www.cbs.dtu.dk/services/TMHMM/>).

### Construction of plasmids and different types of bacterial strains

To construct *petL*<sup>PM</sup>-bearing Enterobacteriaceae, full-length *petL* of *P. multocida* HuN001 (GenBank accession no. CP073238) (Lin et al. 2021) was amplified using the primers pPBA-HindIII-F/pPBA-Sac I-R or pMD19-Sal I-F/pMD19-Sac I-R, as shown in Table 1, and subsequently cloned and inserted into pBA1101 and pMD<sub>19</sub>-T to generate the recombinant plasmids pPBA-*petL*<sup>PM</sup> and

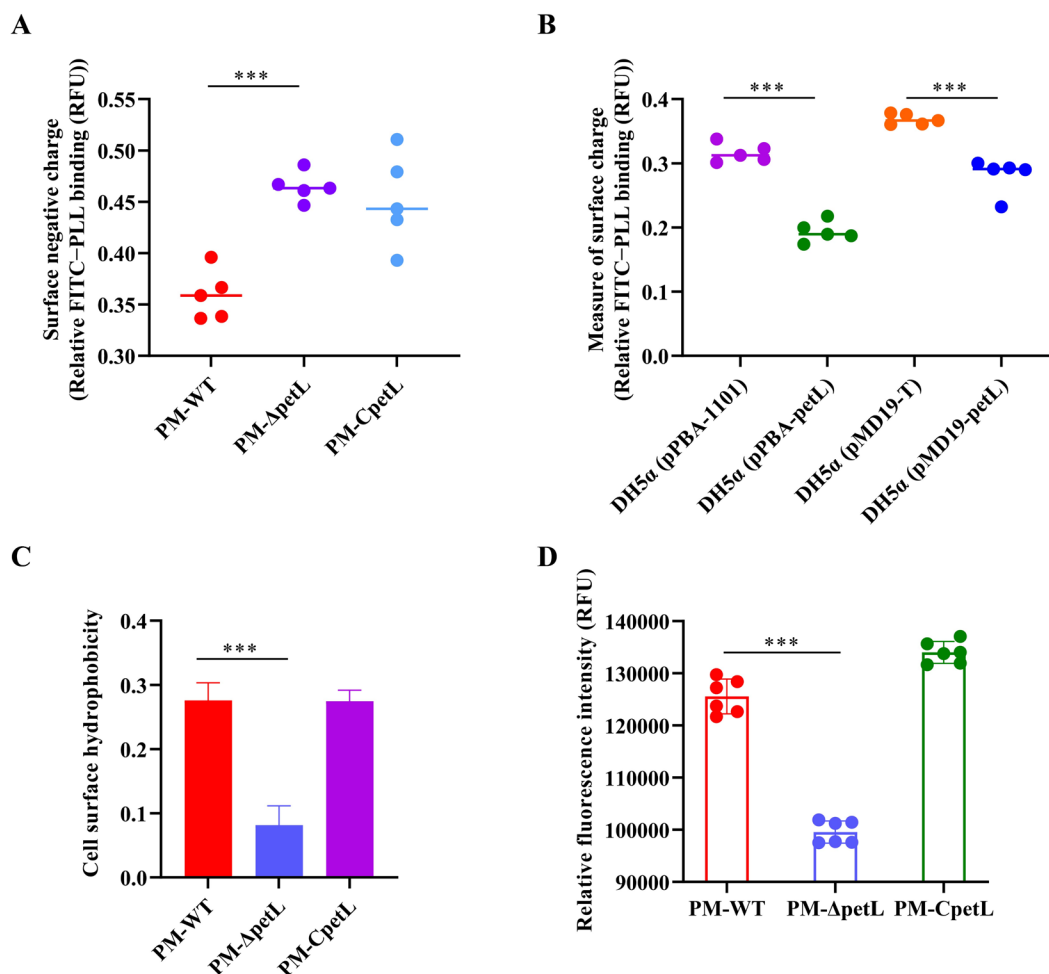


**Fig. 4** Characteristics of the *Pasteurella multocida* wild-type strain (PM-WT), *petL* deletion strain (PM-Δ*petL*), and *petL* complementation strain (PM-C*petL*). **A** Membrane surface-negative charges of PM-WT, PM-Δ*petL* and PM-C*petL*; **B** membrane surface-negative charges of *E. coli* strains harboring *petL* from *P. multocida*; **C** cell surface hydrophobicity of PM-WT, PM-Δ*petL* and PM-C*petL*; **D** cell permeability of PM-WT, PM-Δ*petL* and PM-C*petL*

pMD-*petL*<sup>PM</sup>, respectively. These recombinant plasmids were subsequently transformed into *E. coli* DH5α (pPBA-*petL*<sup>PM</sup> and/or pMD-*petL*<sup>PM</sup>), MG1655 (pPBA-*petL*<sup>PM</sup>), and *K. pneumoniae* (pPBA-*petL*<sup>PM</sup>) strains.

Our previously reported protocol (Lv et al. 2023) was followed to construct the *P. multocida petL*-deletion strain (PM-Δ*petL*). Briefly, the upstream and downstream fragments of *petL* were amplified using the genomic DNA of *P. multocida* HuN001 as a template with primers (petL-L-RH-F/petL-L-RH-R, petL-R-RH-F/petL-R-RH-R), as shown in Table 1. The fragments were ligated together by overlap PCR and cloned and inserted into the plasmid pSHK5(TS)-*NgAgo* (Fu et al. 2019) to generate the plasmid pSHK-Δ*petL*, which was subsequently transformed into competent *P. multocida* HuN001 cells by electroporation (2500 V, 25 μF, 600 Ω). *P. multocida* cells were incubated in prewarmed tryptic soy broth

(TSB; Becton, Dickinson and Company, USA) supplemented with 5% newborn bovine serum (NBS; Tianhang, Hangzhou, China) and shaken at 180 rpm and 28°C for 3 h. Afterwards, the bacterial culture mixture was centrifuged at 6000 rpm for 15 min, and the pellets were suspended in 100 μL of TSB supplemented with 10% NBS. Finally, the suspensions were plated on tryptic soy agar (TSA) supplemented with 5% NBS and kanamycin (50 μg/mL final concentration), followed by incubation at 28°C for 48 h. Single colonies were picked, and the occurrence of the first crossover event was confirmed by PCR with primers petL-outer-JD-F/petL-outer-JD-R. Colonies with correct profiles were incubated on TSA containing 5% NBS at 42°C overnight to accelerate the occurrence of the second crossover event. The deletion of *petL* was finally confirmed by PCR with the primers petL-inner-JD-F/petL-inner-JD-R and was double

**Table 1** Bacterial strains, plasmids and primers used in this study

Bacterial strain	Characteristics	Sources
HuN001	Wild-type <i>P. multocida</i> strain, capsular type A	Our laboratory
PM-ΔpetL	<i>petL</i> -deletion strain of HuN001	This study
PM-CpetL	<i>petL</i> -complementary strains	This study
KP01	Wild-type <i>K. pneumoniae</i> strain from pigs	Our laboratory
KP02	Wild-type <i>K. pneumoniae</i> strain from pigs	Our laboratory
DH5α	<i>E. coli</i> strain	YIBAI
MG1655	<i>E. coli</i> K12 strain	ANGYUBIO
<b>Plasmids</b>		
pSHK5Ts-NgAgo	NgAgo and RBS gene insert between the Kan promoter and Kanr gene of temperature-sensitive plasmid pSHK5Ts, can express NgAgo protein; Kan <sup>r</sup>	Gifted by Anding Zhang
pPBA1101	<i>E. coli</i> - <i>P. multocida</i> shuttle vector, Kan <sup>r</sup>	Gifted by John Boyce
pMD19-T	Cloning vector; Amp <sup>r</sup>	TAKARA
pSHK5Ts-ΔpetL	<i>petL</i> upstream and downstream fragment amplified from HuN001 ligated into pSHK5Ts-NgAgo; Kan <sup>r</sup>	This study
pPBA1101-petL	pPBA1101 containing <i>petL</i> ; Kan <sup>r</sup>	This study
pMD19-T-petL	pMD19-T containing <i>petL</i> ; Amp <sup>r</sup>	This study
<b>Primers</b>		
Primers	Sequences (5'~3')	Product size
petL-F	ATGAAAAAATTACGATTTTCGTT	<i>petL</i> full length (1,632 bp)
petL-R	CTAGCGTATGCGACAAC	
petL-L-RH-F	CGCGGATCCAATTTCGATGCCTTTCTCATCAGT	<i>petL</i> upstream fragment (821 bp)
petL-L-RH-R	TAGGAGTTTTGTTGTTATAGGACATTGAATAAAAGCCAAGTAAAG	
petL-R-RH-F	TTTATCAATGTCTATAACAACAAAACCTCTAAAAAATCGACT	<i>petL</i> downstream fragment (890 bp)
petL-R-RH-R	CGGGGTACCAAGGTATTGGGCAACAGTTAGT	
petL-inner-JD-F	AATCTGGCAGAAGGTTC A	Identification of <i>petL</i> deletion (438 bp)
petL-inner-JD-R	GGTGGTTTGTGCTCATA	
petL-outer-JD-F	ACTGGATTACGCCGTTTGTGTTGA	Identification the recombinant of <i>petL</i> (wild type: 4,100 bp; mutant type: 2,468 bp)
petL-oute-JD-F	TCCACCGAAAACACAATCTTGCC	
100-q-petL-F	CCGTTATTAGCAAATCGGGGCG	qPCR for <i>petL</i>
100-q-petL-R	ATCTGGAACATACAGGGGAC	
q-aroA-F	ACACCGAACAAAGGAAGGCAA	qPCR for <i>aroA</i>
q-aroA-R	TCTGCGCCAGCTTGACATAA	
pPBA-HindIII-F	CCCAAGCTTGATGAAAAAATTACGATTCGTTGGTCTTTA ( <i>HindIII</i> )	<i>petL</i> full length (1,632 bp)
pPBA-Sac I-R	CCCGAGCTCCTAGCGTATGCGACAACGA ( <i>SacI</i> )	
pMD19-Sal I-F	ACGCGTCGACGATGAAAAAATTACGATTCGTTGGTCTTTA ( <i>Sall</i> )	<i>petL</i> full length (1,632 bp)
pMD19-Sac I-R	CCCGAGCTCCTAGCGTATGCGACAACGA ( <i>SacI</i> )	

confirmed by Sanger sequencing. To construct complementary strains (PM-CpetL), full-length *petL* was amplified via PCR with the primers pPBA-HindIII-F/pPBA-Sac I-R and subsequently cloned and inserted into pPBA1101 to generate the transforming plasmid pPBA-*petL*, which was subsequently transformed into competent PM-ΔpetL cells via electroporation.

#### Antimicrobial susceptibility testing (AST)

MIC values were measured by the broth microdilution method following the guidelines published by CLSI

(CLSI 2018). Briefly, Mueller–Hinton broth (Sigma–Aldrich, St. Louis, US) containing a series of twofold dilutions of colistin (MedChemExpress, Monmouth Junction, US) ranging from 64 μg/ml to 0.0625 μg/mL was seeded into wells (100 μL per well) in different columns of a 96-well plate (Corning, Corning, US). In parallel, bacterial strains (*P. multocida*, *E. coli*, or *K. pneumoniae*) were prepared by suspending overnight cultures on Mueller–Hinton agars in sterile normal saline to a turbidity of 0.5 McFarland standard. Afterwards, an additional 100-fold dilution was applied to the bacterial suspensions, which

were added to the wells (100  $\mu$ L per well) of the above-mentioned plates containing different concentrations of colistin. The control wells included those containing Mueller–Hinton broth only (200  $\mu$ L per well) and/or those containing 100  $\mu$ L of broth plus 100  $\mu$ L of bacterial suspension. The plate was then incubated at 37°C overnight, and parallel tests were performed to confirm the results. The CLSI breakpoint of colistin (2  $\mu$ g/mL) was used for the interpretation of the testing results for *E. coli* and *K. pneumoniae*. *E. coli* ATCC25922 was used as a quality control.

#### Measurement of growth curves

Overnight cultures of *P. multocida* wild-type (PM-WT) and PM- $\Delta$ petL strains were inoculated into fresh TSB supplemented with 5% NBS at a ratio of 1:100 ( $v/v$ ). Thereafter, each of the bacterial inoculations (200  $\mu$ L) was added to different wells of a 96-well plate (JET BIO-FIL, Guangzhou, China). Growth curves for different bacterial strains were generated by measuring the OD<sub>600</sub> values every 1 h for 24 h using a fast automatic growth analyzer (OyGrowth Curves Ab Ltd., Finland). The experiments were repeated three times.

#### Measurement of bacterial surface hydrophobicity

Bacterial surface hydrophobicity was determined as previously described (Wang et al. 2014). Briefly, overnight cultures of PM-WT, PM- $\Delta$ petL, and PM-CpetL in TSB containing 5% NBS were centrifuged at 6000 rpm for 5 min. Pellets were washed twice using PBS (pH=7.4) and resuspended to an OD<sub>600</sub> of 1.0, which was recorded as A<sub>0</sub>. Thereafter, 5 mL of bacterial culture was mixed thoroughly with 2 mL of xylene, followed by standing for 60 min at room temperature. After that, the OD<sub>600</sub> of the aqueous phase after extraction with xylene was also measured and recorded as A. The hydrophobicity of the bacterial cells was calculated as  $[(A_0 - A)/A_0] \times 100$  (Wang et al. 2014). The experiments were repeated three times.

#### Determination of outer membrane permeability

OM permeability was determined following a previously described method (Li et al. 2023). Briefly, overnight cultures of PM-WT, PM- $\Delta$ petL and PM-CpetL in TSB containing 5% NBS were centrifuged at 6000 rpm for 5 min. The pellets were washed twice with PBS (pH=7.4) and resuspended to an OD<sub>600</sub> of 0.5. Afterwards, 1.92 mL of bacterial suspension and 80  $\mu$ L of *N*-phenyl-1-naphthylamine (NPN, Sigma–Aldrich, St. Louis, US) solution (1 mM) were mixed rapidly. Changes in fluorescence intensity were measured using an EnSpire® Multimode Plate Reader (PerkinElmer, Waltham, US). The excitation

and emission wavelengths were 350 nm and 428 nm, respectively. For each bacterial strain, five parallel tests were performed, and instruments calibrated with PBS were included as controls.

#### Measurement of surface negative charges

Bacterial membrane surface charges were measured as described previously (Jangir et al. 2022). Briefly, overnight cultures of PM-WT, PM- $\Delta$ petL and PM-CpetL in TSB containing 5% NBS were centrifuged at 6000 rpm for 5 min. Pellets were washed twice using PBS (pH=7.4) and resuspended to an OD<sub>600</sub> of 0.1. Instruments calibrated with PBS were included as controls. Next, FITC-labeled poly-L-lysine (Sigma-Aldrich) was added (final concentration: 6.5  $\mu$ g/mL) and incubated at room temperature for 10 min. After centrifugation at 6000 rpm for 5 min, the supernatants were collected to measure the changes in fluorescence intensity using an EnSpire® Multimode Plate Reader (PerkinElmer). The excitation and emission wavelengths were 500 nm and 530 nm, respectively. Membrane surface negative charges were quantified as previously described (Jangir et al. 2022).

#### LPS extraction and SDS polyacrylamide gel electrophoresis (SDS–PAGE)

LPSs of different bacterial strains were extracted using a commercial LPS Extraction Kit (iNtRON, Seongnam, South Korea) and separated using SDS polyacrylamide gel electrophoresis (SDS-PAGE). Afterwards, the gel was fixed in a prepared fixative solution (30 mL of anhydrous ethanol+10 mL of glacial acetic acid+40 mL of double steaming water) and shaken at 180 rpm overnight at room temperature. The solution was then discarded, and 100 mL of periodic acid solution (7 mg/mL) was added. Following shaking at 180 rpm for 10 min at room temperature, the gel was washed three times with 100 mL of double steaming water and stained with silver nitrate solution (1 mg/mL) for 30 min at room temperature. Finally, the gel was treated with 30 mg/mL sodium carbonate solution plus 0.02% formaldehyde for 20 min until the bands appeared. The reaction was stopped by the addition of 10% glacial acetic acid.

#### Lipid A extraction and analysis

Bacterial LPS-lipid A was isolated and purified for MALDI-TOF–MS analysis as previously described (Sun et al. 2017). Briefly, bacterial strains in the mid-log phase were inoculated on TSA supplemented with 0.8 mM IPTG and 1  $\mu$ g/mL colistin and incubated at 37°C for 16–18 h. Bacterial colonies were subsequently washed with 10 mL of Tris-HCl buffer (30 mM, pH 8.1) and subsequently centrifuged at 4°C and 5000 rpm for 15 min. The resulting pellets were subsequently resuspended in



400  $\mu$ L of Tris-HCl (30 mM, pH 8.1) solution containing 20% sucrose and treated with 40  $\mu$ L of lysozyme (1 mg/mL), followed by incubation in an ice bath for 30 min. The resulting bacterial suspensions were subsequently stored at  $-80^{\circ}\text{C}$  for 30 min and melted at room temperature. This process was repeated twice. Then, the bacterial suspensions were mixed with 5 mL of EDTA (3 mM) and sonicated for 4 min (sonicating for one second and stopping for 3 s). The products were centrifuged at  $4^{\circ}\text{C}$  and 5000 rpm for 15 min, followed by centrifugation of the supernatants at  $4^{\circ}\text{C}$  and 16,800 rpm for 60 min to harvest the LPS. To obtain lipid A, the prepared LPS was dissolved in 200  $\mu$ L of Tris-HCl solution (30 mM, pH 8.1) containing 0.2% SDS, which was then treated with RNase I (25  $\mu\text{g}/\text{mL}$ ) and DNase I (100  $\mu\text{g}/\text{mL}$ ) at  $37^{\circ}\text{C}$  for 2 h. The product was then treated with protease K (100  $\mu\text{g}/\text{mL}$ ) at  $37^{\circ}\text{C}$  for another 2 h, followed by heating at  $100^{\circ}\text{C}$  for 1 h. Thereafter, 200  $\mu$ L of acidified ethanol solution (20 mL of 95% ethanol mixed with 100  $\mu$ L of 4 M HCl) was added, and the mixture was mixed thoroughly. The mixture was then centrifuged at 5000 rpm for 5 min to harvest the pellets, which were then washed twice with 200  $\mu$ L of 95% ethanol, followed by washing with 200  $\mu$ L of absolute ethyl alcohol. Finally, lipid A was dissolved in 20  $\mu$ L of chloroform-methanol solution (2/1, v/v). The extracted lipid A was extensively analyzed by MALDI-TOF-MS.

### Statistical analysis

Statistical analysis was performed using multiple t tests in GraphPad Prism 8.0 (GraphPad Software, San Diego, CA). The data are presented as the means  $\pm$  standard deviations (SD). The significance level was set at a *P* value of  $<0.05$  (\*), a *P* value of  $<0.01$  (\*\*), or a *P* value of  $<0.001$  (\*\*\*)

### Abbreviations

LPS	Lipopolysaccharide
MALDI-TOF-MS	Matrix-assisted laser desorption ionization time-of-flight mass spectrometry
MCR	Mobile-colistin-resistant
MDR	Multidrug resistant
MIC	Minimum inhibitory concentration
PDR	Pan drug resistant
PEtn	Phosphoethanolamine
XDR	Extensive drug resistant

### Acknowledgements

We thank Prof. Anding Zhang (Huazhong Agricultural University, Wuhan, China) for the gift of the plasmid pSHK5(TS)-NgAgo and Prof. John D. Boyce (Monash University, Melbourne, Australia) for the gift of the plasmid pPBA1101.

### Authors' contributions

Conceptualization: ZP, JY, and BW. Investigation and methodology: JY, LL, HB, QL, CS, LH. Writing: ZP, and JY. Editing: ZP, BW, and HC. Funding acquisition and supervision: ZP and BW. All authors have read and agreed to the final version of the manuscript.

### Funding

This work was supported in part by the Hubei Provincial Natural Science Foundation of China (grant no. 2023AFA094), the Yingzi Tech & Huazhong Agricultural University Intelligent Research Institute of Food Health (No. IRIFH202209), Fundamental Research Funds for the Central Universities (Project 2662023PY005), and the Hubei Hongshan Laboratory & Huazhong Agricultural University Start-up Fund. The funders had no role in the study design, data collection and interpretation, or the decision to submit the work for publication.

### Availability of data and materials

Not applicable.

### Declarations

#### Ethics approval and consent to participate

Not applicable.

#### Consent for publication

Not applicable.

#### Competing interests

The authors declare that they have no competing interests. Authors Huan-chun Chen and Zhong Peng were not involved in the journal's review or decisions related to this manuscript.

Received: 18 January 2024 Accepted: 8 March 2024

Published online: 03 April 2024

### References

- Anandan, A., G.L. Evans, K. Condic-Jurkic, M.L. O'Mara, C.M. John, N.J. Phillips, G.A. Jarvis, S.S. Wills, K.A. Stubbs, I. Moraes, et al. 2017. Structure of a lipid A phosphoethanolamine transferase suggests how conformational changes govern substrate binding. *Proc Natl Acad Sci U S A* 114: 2218–2223. <https://doi.org/10.1073/pnas.1612927114>.
- CLSI. 2018. *Performance standards for antimicrobial susceptibility testing. M100, 28th Edition*.
- El-Demerdash, A.S., R.E. Mowafy, H.A. Fahmy, A.A. Matter, and M. Samir. 2023. Pathognomonic features of *Pasteurella multocida* isolates among various avian species in Sharkia Governorate, Egypt. *World J Microbiol Biotechnol* 39: 335. <https://doi.org/10.1007/s11274-023-03774-2>.
- Fu, L., C. Xie, Z. Jin, Z. Tu, L. Han, M. Jin, Y. Xiang, and A. Zhang. 2019. The prokaryotic Argonaute proteins enhance homology sequence-directed recombination in bacteria. *Nucleic Acids Research* 47: 3568–3579. <https://doi.org/10.1093/nar/gkz040>.
- Harper, M., and J.D. Boyce. 2017. The myriad properties of *Pasteurella multocida* lipopolysaccharide. *Toxins (Basel)* 9: 254. <https://doi.org/10.3390/toxin9080254>.
- Harper, M., A.D. Cox, B. Adler, and J.D. Boyce. 2011. *Pasteurella multocida* lipopolysaccharide: The long and the short of it. *Veterinary Microbiology* 153: 109–115. <https://doi.org/10.1016/j.vetmic.2011.05.022>.
- Harper, M., A. Wright, F. St Michael, J. Li, D. Deveson Lucas, M. Ford, B. Adler, A.D. Cox, and J.D. Boyce. 2017. Characterization of two novel lipopolysaccharide phosphoethanolamine transferases in *Pasteurella multocida* and their role in resistance to cathelicidin-2. *Infection and Immunity* 85: 10–128. <https://doi.org/10.1128/iai.00557-17>.
- Huang, J., Y. Zhu, M.L. Han, M. Li, J. Song, T. Velkov, C. Li, and J. Li. 2018. Comparative analysis of phosphoethanolamine transferases involved in polymyxin resistance across 10 clinically relevant gram-negative bacteria. *International Journal of Antimicrobial Agents* 51: 586–593. <https://doi.org/10.1016/j.ijantimicag.2017.12.016>.
- Jangir, P.K., Q. Yang, L.P. Shaw, J.D. Caballero, L. Ogunlana, R. Wheatley, T. Walsh, and R.C. MacLean. 2022. Preexisting chromosomal polymorphisms in pathogenic *E. coli* potentiate the evolution of resistance to a last-resort antibiotic. *Elife* 11: e78834. <https://doi.org/10.7554/elife.78834>.

- Kempf, I., E. Jouy, and C. Chauvin. 2016. Colistin use and colistin resistance in bacteria from animals. *International Journal of Antimicrobial Agents* 48: 598–606. <https://doi.org/10.1016/j.ijantimicag.2016.09.016>.
- Li, X., J. Zhou, R. Han, F. Yu, K. Liu, M. Zhao, Y. Liu, Z. Xue, and S. Zhao. 2023. Phosphatase A1 accessory protein PlaS from *Serratia marcescens* controls cell membrane permeability, fluidity, hydrophobicity, and fatty acid composition in *Escherichia coli* BL21. *International Journal of Biological Macromolecules* 253: 126776. <https://doi.org/10.1016/j.ijbiomac.2023.126776>.
- Lin, L., C. Li, F. Wang, X. Wang, Y. Zhang, S. Liu, W. Liang, L. Hua, Z. Peng, and B. Wu. 2021. Complete genome sequence of *Pasteurella multocida* HuN001, a capsular type A strain from a human. *Microbiology Resource Announcements* 10: e0039521. <https://doi.org/10.1128/mra.00395-21>.
- Liu, Y.Y., Y. Wang, T.R. Walsh, L.X. Yi, R. Zhang, J. Spencer, Y. Doi, G. Tian, B. Dong, X. Huang, et al. 2016. Emergence of plasmid-mediated colistin resistance mechanism MCR-1 in animals and human beings in China: a microbiological and molecular biological study. *The Lancet Infectious Diseases* 16: 161–168. [https://doi.org/10.1016/s1473-3099\(15\)00424-7](https://doi.org/10.1016/s1473-3099(15)00424-7).
- Lv, Q., Y. Shang, H. Bi, J. Yang, L. Lin, C. Shi, M. Wang, R. Xie, Z. Zhu, F. Wang, et al. 2023. Identification of two-component system ArcAB and the universal stress protein E in *Pasteurella multocida* and their effects on bacterial fitness and pathogenesis. *Microbes and Infection* :105235. <https://doi.org/10.1016/j.micinf.2023.105235>.
- Michael, G.B., J.T. Bossé, and S. Schwarz. 2018. Antimicrobial resistance in *Pasteurellaceae* of veterinary origin. *Microbiology Spectrum* 6. <https://doi.org/10.1128/microbiolspec.arba-0022-2017>.
- Peng, Z., L. Lin, X. Wang, H. Chen, and B. Wu. 2022. The public health concern of *Pasteurella multocida* should not be ignored. *Lancet Microbe* 3: e560. [https://doi.org/10.1016/s2666-5247\(22\)00152-5](https://doi.org/10.1016/s2666-5247(22)00152-5).
- Piorunek, M., B. Brajer-Luftmann, and J. Walkowiak. 2023. *Pasteurella multocida* infection in humans. *Pathogens* 12 (10): 1210. <https://doi.org/10.3390/pathogens12101210>.
- Poirel, L., A. Jayol, and P. Nordmann. 2017. Polymyxins: antibacterial activity, susceptibility testing, and resistance mechanisms encoded by plasmids or chromosomes. *Clinical Microbiology Reviews* 30: 557–596. <https://doi.org/10.1128/cmr.00064-16>.
- Sebbar, G., S. Fellahi, A. Filali-Maltouf, and B. Belkadi. 2020. Detection of colistin resistance in mannheimia hemolytica & *Pasteurella multocida* isolates from ruminants in Morocco. *Pakistan Veterinary Journal* 41: 127–131. <https://doi.org/10.29261/pakvetj/2020.077>.
- Seethalakshmi, P.S., R. Rajeev, A. Prabhakaran, G.S. Kiran, and J. Selvin. 2023. The menace of colistin resistance across globe: Obstacles and opportunities in curbing its spread. *Microbiological Research* 270: 127316. <https://doi.org/10.1016/j.micres.2023.127316>.
- Sharma, J., D. Sharma, A. Singh, and K. Sunita. 2022. Colistin resistance and management of drug resistant infections. *Canadian Journal of Infectious Diseases and Medical Microbiology* 2022: 4315030. <https://doi.org/10.1155/2022/4315030>.
- Sun, J., Y. Xu, R. Gao, J. Lin, W. Wei, S. Srinivas, D. Li, R.S. Yang, X.P. Li, X.P. Liao, et al. 2017. Deciphering MCR-2 colistin resistance. *mBio* 8: 10–128. <https://doi.org/10.1128/mbio.00625-17>.
- Walsh, T.R., A.C. Gales, R. Laxminarayan, and P.C. Dodd. 2023. Antimicrobial rResistance: addressing a global threat to humanity. *PLoS Medicine* 20: e1004264. <https://doi.org/10.1371/journal.pmed.1004264>.
- Wang, J., W. Ma, Z. Wang, Y. Li, and X. Wang. 2014. Construction and characterization of an *Escherichia coli* mutant producing Kdo<sub>2</sub>-lipid A. *Marine Drugs* 12: 1495–1511. <https://doi.org/10.3390/md12031495>.
- WHO. 2018. *Critically important antimicrobials for human medicine: 6th revision*. <https://iris.who.int/bitstream/handle/10665/312266/9789241515528-eng.pdf?sequence=1>. Accessed 7 Oct 2023.
- Wilkie, I.W., M. Harper, J.D. Boyce, and B. Adler. 2012. *Pasteurella multocida*: Diseases and pathogenesis. *Current Topics in Microbiology and Immunology* 361: 1–22. [https://doi.org/10.1007/82\\_2012\\_216](https://doi.org/10.1007/82_2012_216).
- Wilson, B.A., and M. Ho. 2013. *Pasteurella multocida*: From zoonosis to cellular microbiology. *Clinical Microbiology Reviews* 26: 631–655. <https://doi.org/10.1128/cmr.00024-13>.

## Publisher's Note

Springer Nature remains neutral with regard to jurisdictional claims in published maps and institutional affiliations.